UMRSF-TDDFT: Unrestricted Mixed-Reference Spin-Flip-TDDFT†

Konstantin Komarov,‡ Minseok Oh,¶ Hiroya Nakata,§ Seunghoon Lee,*,¶ and Cheol Ho Choi*,‖

‡*Center for Quantum Dynamics, Pohang University of Science and Technology, Pohang 37673, South Korea*

¶*Department of Chemistry, Seoul National University, Seoul 151-747, South Korea*

§*Idemitsu Kosan Co.,Ltd, Tokyo 100-832, Japan*

‖*Department of Chemistry, Kyungpook National University, Daegu 41566, South Korea*

E-mail: seunghoonlee@snu.ac.kr; cchoi@knu.ac.kr

†Prof. Massimo Olivucci Festschrift

Abstract

An unrestricted version of Mixed-Reference Spin-Flip Time-Dependent Density Functional Theory (UMRSF-TDDFT) was developed based on unrestricted Kohn-Sham orbitals (UKS) with a new molecular orbital (MO) reordering scheme. Additionally, a simple yet accurate method for estimating $\langle S^2 \rangle$ expectation values was devised. UMRSF-TDDFT was benchmarked against cases where DFT, TDDFT, and SF-TDDFT traditionally fail to provide accurate descriptions. In an application to the ground and excited states of a Be atom, UMRSF-TDDFT successfully recovers the degenerate states, with its energies slightly reduced compared to its RO counterpart, due to the additional variational flexibility of UKS. A clear difference between UMRSF and U-SF-TDDFT is evident in the bond breaking of the hydrogen fluoride system, as the latter misses an important configuration. In the case of the Jahn-Teller distortion of trimethylenemethane (TMM), the relative singlet energy compared to the triplet is lower by 0.1 eV and 0.2 eV for UMRSF and U-SF-TDDFT, respectively, than that of MRSF-TDDFT. The reduction in UMRSF energy is attributed to spatial orbital relaxations, whereas the reduction in U-SF-TDDFT energy results from spin contamination. Overall, the additional orbital relaxations afforded by unrestricted Kohn-Sham (UKS) orbitals in UMRSF-TDDFT lead to lower total system energies compared to their restricted open-shell counterparts. This enhancement adds a practical and accurate quantum chemical theory to the existing RO variant for addressing challenging systems where traditional quantum theories suffer.

TOC Graphic

Keywords

Unrestricted, Mixed-Reference, Spin-Flip, DFT, TDDFT, MRSF-TDDFT

Introduction

Density Functional Theory (DFT) and Time-Dependent Density Functional Theory (TDDFT) are the primary tools for general applications involving ground and excited electronic states, respectively. However, the single-reference formulation of DFT imposes significant limitations on systems with multi-configurational characteristics, such as open-shell singlet cases including diradicals and bond-breaking events.[1,2] TDDFT also has well-known inherent failures in describing the energy of long-range charge transfer excitations,[3–7] excited states with substantial double excitation character,[8–11] excited states of molecules undergoing bond breaking,[12,13] and the topology of conical intersections (CIs).[11,14–17]

Perhaps, the correct description of conical intersections (CIs) is one of the most challenging requirements of electronic structure theory, as it should produce non-vanishing nonadiabatic coupling between the intersecting states. Surprisingly, this requirement for the S_1/S_0 CIs is violated by most single-reference theories including single-state multi-reference computational methods[16,16,18–27] such as single-state (SS)-CASPT2.[16,18,19] Multi-State multi-reference computational methods[20–24] are capable of producing the correct topology of CIs,[16,25–27] however at the expense of very high cost of computations. A solution to this problem is to develop a unified and efficient quantum mechanical theory that can accurately describe both ground and excited electronic states on an equal footing.

To address these challenges, a new quantum theory, Mixed-Reference Spin-Flip Time-Dependent Density Functional Theory (MRSF-TDDFT; MRSF for brevity), has been developed.[28,29] MRSF is a versatile platform that incorporates both the static multi-configurational effect and dynamical electron correlation into the description of the ground and excited electronic states within the computationally efficient linear response theory.[2,28,30–35] In a series of studies,[2,31–40] it has been demonstrated that the MRSF approach can yield accurate nonadiabatic coupling matrix elements (NACMEs),[2,36] enabling reliable nonadiabatic molecular dynamics (NAMD) simulations.[34,41–46] Additionally, MRSF provides a topologically correct description of conical intersections,[33,35,39] accurate values of singlet–triplet gaps,[32,37] accurate spin-orbit

couplings (SOC),[47] and very accurate X-ray absorption predictions.[48] This method has also been successfully used in designing high-performance optoelectronic materials.[39,49–51] A perspective further underscores the merits of MRSF in this context.[52] Recent efforts to optimize exchange-correlation (XC) functionals specifically designed for MRSF can further improve its performance.[47,53]

The essence of MRSF lies in the utilization of responses from two components of the triplet state,[28] as opposed to the single-component formulation of SF-TDDFT.[54–56] This doubles the response space without introducing multi-reference orbital optimization found in Multiconfiguration Pair-Density Functional Theory (MC-PDFT),[57] or requiring expensive high-rank excitations from a single reference, as in Spin-Adopted (SA) SF-DFT.[58] Due to its formulation, MRSF recovers important double excitations, addressing the primary issue of missing doubly excited states in TDDFT[59–61] without incurring the high computational cost associated with full doubles. As a result, MRSF maintains the efficiency of linear response theory with simple single-reference orbital optimization while leveraging the advantages of multi-reference theories, making it both practical and potentially accurate.

For its realization, a new mixed-reference state that has an equiensemble density of the M_S = +1 and $M_S = -1$ components of a triplet state was introduced as,

$$\rho_0^{\mathrm{MR}}(x) = \frac{1}{2}\left\{\rho_0^{M_S=+1}(x) + \rho_0^{M_S=-1}(x)\right\}. \tag{1}$$

This symmetric utilization of the two states ($M_s = \pm 1$) of the triplet allows us to address the problematic spin contamination of SF-TDDFT[56] through a formulational structure, which we call "external contraction." By pre-defining the equations of motion for each spin state, we eliminate the need to identify them individually. As MRSF utilizes the triplet reference state, both the ground singlet and all excited singlet states can be obtained on an equal footing. This approach not only eliminates the general topological problem of conical intersections[33,35,39] present in all single-reference theories but also allows for the description of open-shell ground singlet states, such as diradicals and Jahn-Teller

distortions,[32,37] as well as bond-breaking events.[2]

The current implementation of MRSF-TDDFT is based on a restricted open-shell Kohn-Sham (ROKS) formalism, chosen for its simplicity and freedom from spin contamination and orbital asymmetries between α and β orbitals. In contrast, the unrestricted Kohn-Sham (UKS) approach offers the advantage of variational flexibility, as both α and β orbitals are independently optimized. Generally, MRSF-TDDFT based on UKS is expected to be more adaptable in various strongly correlated situations compared to ROKS formulations. The development of this approach is the main focus of the current paper.

Since the concept of MRSF is based on the non-conventional approach of an equiensemble density, understanding its potential is not straightforward. Therefore, this paper also aims to provide detailed, pedagogical explanations of the entire MRSF process using some simple yet challenging systems.

Introducing UMRSF-TDDFT

As the general description of MRSF-TDDFT using restricted open-shell (RO) mixed reference can be found elsewhere,[28,29] only the main aspects of the unrestricted Kohn-Sham (KS) DFT version of MRSF-TDDFT (UMRSF-TDDFT; UMRSF for brevity) shall be presented here. As discussed in the Introduction, a new mixed reference has been introduced whose density (ρ_0^{MR}) is the equiensemble density of the M_S = +1 and $M_S = -1$ components of a triplet state as shown in Eq. 1. Two open-shell molecular orbitals of the new mixed reference are defined by novel $+$ and $-$ spin functions.[28]

$$+ = \frac{(1+i)\alpha + (1-i)\beta}{2} \tag{2a}$$

$$- = \frac{(1-i)\alpha + (1+i)\beta}{2}, \tag{2b}$$

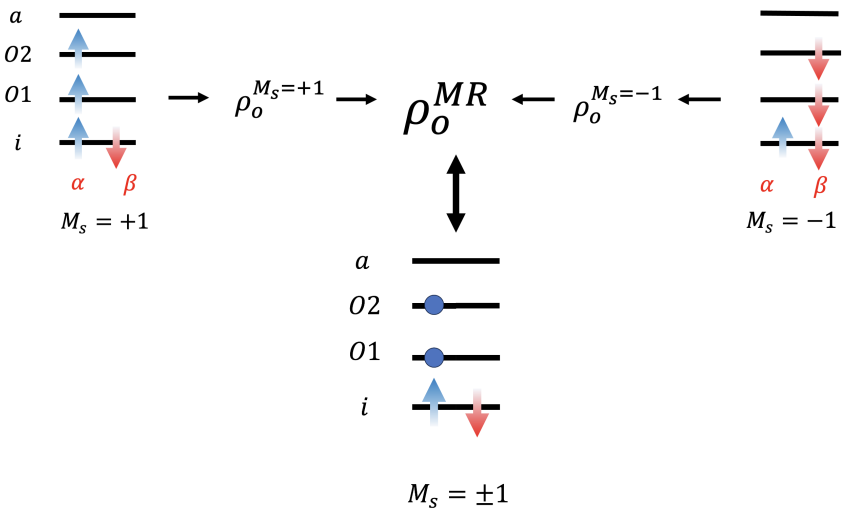

(a)

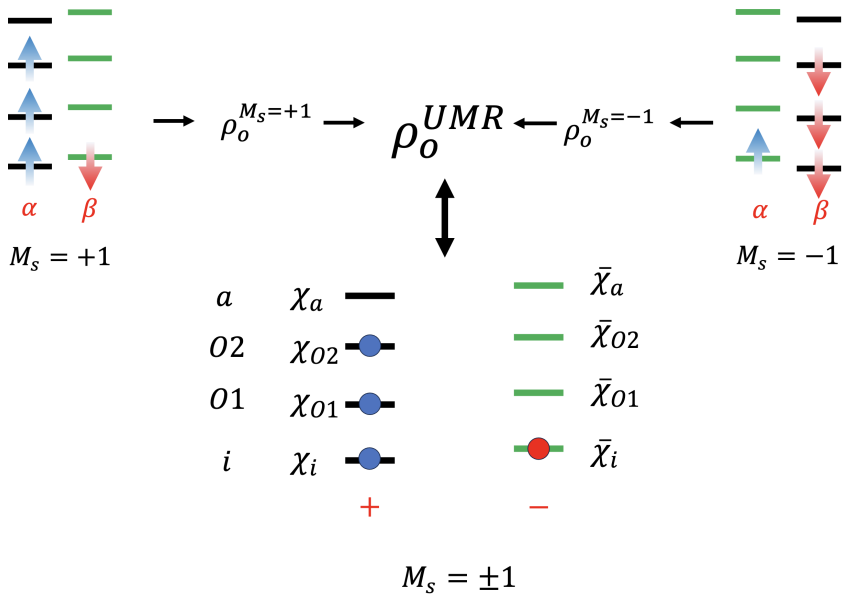

(b)

Figure 1: The concepts of hypothetical single references for (a) restricted open-shell Kohn-Sham (ROKS) and (b) unrestricted Kohn-Sham (UKS) cases.

where i is the imaginary unit number. The $+$ and $-$ spin functions are represented as blue and red dots in Fig. 1, where the regular α and β spin functions are represented by blue and red arrows. It is noted that two $+$ electrons (blue dots) are particularly adopted in the mixed reference (bottom panel in Fig. 1(a)), since it can be readily shown that the

final equations are identical even if two $-$ electrons are chosen.

As in ROKS, a new mixed reference for UKS is introduced in the current study whose density (ρ_0^{UMR}) is the equiensemble density of the M_S = +1 and $M_S = -1$ components of a triplet state as

$$\rho_0^{\mathrm{UMR}}(x) = \frac{1}{2}\left\{\rho_0^{M_S=+1}(x) + \rho_0^{M_S=-1}(x)\right\}. \tag{3}$$

Unlike ROKS, now the spatial parts of α (black) and β (green) orbitals are different in UKS. It should be noted that the spatial part of α (black) orbitals of $\mathrm{M}_S = +1$ state is identical to the β (black) orbitals of $\mathrm{M}_S = -1$ and vise versa. To be consistent, the black and green spatial orbitals are designated as χ and $\bar{\chi}$, respectively as shown in Fig. 1(b). The corresponding $\mathrm{M}_S = +1$ and -1 unrestricted references can be written as

$$|\Psi_{\mathrm{Ref}}^{\mathrm{M}_S=+1}\rangle = ||\phi_0^\alpha \bar{\phi}_0^\beta \phi_1^\alpha \bar{\phi}_1^\beta \cdots \phi_{\mathrm{O1}-1}^\alpha \bar{\phi}_{\mathrm{O1}-1}^\beta \phi_{\mathrm{O1}}^\alpha \phi_{\mathrm{O2}}^\alpha\rangle, \tag{4a}$$

$$|\Psi_{\mathrm{Ref}}^{\mathrm{M}_S=-1}\rangle = ||\bar{\phi}_0^\alpha \phi_0^\beta \bar{\phi}_1^\alpha \phi_1^\beta \cdots \bar{\phi}_{\mathrm{O1}-1}^\alpha \phi_{\mathrm{O1}-1}^\beta \phi_{\mathrm{O1}}^\beta \phi_{\mathrm{O2}}^\beta\rangle. \tag{4b}$$

Here, the notation $||\cdots\rangle$ represents a single Slater determinant wherein spin orbitals are defined as $\phi_p^\sigma(x) = \chi_p(\mathbf{r})\sigma(\theta)$ and $\bar{\phi}_p^\sigma(x) = \bar{\chi}_p(\mathbf{r})\sigma(\theta)$ with $\sigma = \alpha, \beta$. The densities of the two references are respectively

$$\rho_0^{M_S=+1}(x) = \sum_{p=1}^{\mathrm{O2}} \phi_p^{\alpha *}(x)\phi_p^\alpha(x) + \sum_{p=1}^{\mathrm{O1}-1} \bar{\phi}_p^{\beta *}(x)\bar{\phi}_p^\beta(x), \tag{5a}$$

$$\rho_0^{M_S=-1}(x) = \sum_{p=1}^{\mathrm{O1}-1} \bar{\phi}_p^{\alpha *}(x)\bar{\phi}_p^\alpha(x) + \sum_{p=1}^{\mathrm{O2}} \phi_p^{\beta *}(x)\phi_p^\beta(x). \tag{5b}$$

In this work, we propose an unrestricted mixed reference of

$$|\Psi_{\mathrm{Ref}}^{\mathrm{UMR}}\rangle = ||\phi_0^+ \bar{\phi}_0^- \phi_1^+ \bar{\phi}_1^- \cdots \phi_{\mathrm{O1}-1}^+ \bar{\phi}_{\mathrm{O1}-1}^- \phi_{\mathrm{O1}}^+ \phi_{\mathrm{O2}}^+\rangle, \tag{6}$$

with the mixed spins, $\sigma = +, -$ defined in Eq. 2. The density of the mixed reference,

$$\rho_0^{\mathrm{UMR}}(x) = \frac{1}{2}\sum_{\sigma=\alpha,\beta}\left[\sum_{p=1}^{\mathrm{O1}-1}\left\{\phi_p^{\sigma*}(x)\phi_p^{\sigma}(x) + \bar{\phi}_p^{\sigma*}(x)\bar{\phi}_p^{\sigma}(x)\right\} + \phi_{\mathrm{O1}}^{\sigma*}(x)\phi_{\mathrm{O1}}^{\sigma}(x) + \phi_{\mathrm{O2}}^{\sigma*}(x)\phi_{\mathrm{O2}}^{\sigma}(x)\right], \tag{7}$$

is an average of the densities for $M_S = \pm 1$ in Eqs. 5a and 5b satisfying the relation in Eq. 3.

By employing the same procedures outlined in Ref. 28, we are able to obtain the singlet and triplet ($k = S, T$) orbital Hessians of the unrestricted mixed reference as

$$A_{pq,rs}^{(k)(0)} = U_{pq}^{(k)}\left\{\delta_{pr}\delta_{qs}(\bar{\epsilon}_q - \epsilon_p) - c_{\mathrm{MRSF}}\,(pr\,|\bar{s}\bar{q}\,)\right\}U_{rs}^{(k)}, \tag{8}$$

where c_{MRSF} denotes the coefficient of the exact Hartree–Fock exchange for the response calculation, $U_{pq}^{(k)}$ is the dimensional transformation introduced in Ref. 29, $(pr|\bar{s}\bar{q})$ is the electron repulsion integral (ERI) defined by

$$(pr|\bar{s}\bar{q}) = \int\int d\mathbf{r}_1 d\mathbf{r}_2 \chi_p^*(\mathbf{r}_1)\bar{\chi}_s^*(\mathbf{r}_2)\frac{1}{|\mathbf{r_1} - \mathbf{r_2}|}\chi_r(\mathbf{r}_1)\bar{\chi}_q(\mathbf{r}_2), \tag{9}$$

and ϵ_p and $\bar{\epsilon}_q$ are the orbital energies defined by

$$\epsilon_p = h_{pp} + V_{pp}^{xc} + \sum_{i=1}^{\mathrm{O1}-1}\left\{(pp|ii) + (pp|\bar{i}\bar{i}) - c_{\mathrm{HF}}(pi|ip)\right\} + \sum_{x=\mathrm{O1,O2}}[(pp\,|xx\,) - c_{\mathrm{HF}}\,(px\,|xp\,)], \tag{10a}$$

$$\bar{\epsilon}_p = \bar{h}_{pp} + \bar{V}_{pp}^{xc} + \sum_{i=1}^{\mathrm{O1}-1}\left\{(\bar{p}\bar{p}|ii) + (\bar{p}\bar{p}|\bar{i}\bar{i}) - c_{\mathrm{HF}}(\bar{p}\bar{i}|\bar{i}\bar{p})\right\} + \sum_{x=\mathrm{O1,O2}}(\bar{p}\bar{p}|xx). \tag{10b}$$

Here, $(pq|rs), (pq|\bar{r}\bar{s}), (\bar{p}\bar{q}|rs)$, and $(\bar{p}\bar{q}|\bar{r}\bar{s})$ represent the ERIs, h_{pq} and $\bar{h}_{pq}$ are the one electron integrals, and V_{pq}^{xc} and $\bar{V}_{pq}^{xc}$ are matrix elements of the first functional derivatives of the exchange-correlation functional with respect to electron density, which involve

various combinations of two sets of spatial orbitals $\{\chi_p\}$ and $\{\bar{\chi}_p\}$. It is noted that c_{HF} is the coefficient for the exact Hartree–Fock exchange for the mean-field (DFT) calculation. Unless otherwise stated in this study, c_{HF} and c_{MRSF} are considered identical, i.e.

$$c_{\mathrm{MRSF}} = c_{\mathrm{HF}}. \tag{11}$$

Because there is no coupling between the responses originating from the two references of the MR-RDM, *a posteriori* coupling was introduced for ROHF in the previous work[28] as

$$A'_{pq,rs} = c_{\mathrm{SPC}} \langle \Psi_{pq}^{\mathrm{M}_S=+1} | \hat{H} | \Psi_{rs}^{\mathrm{M}_S=-1} \rangle \tag{12}$$

where the bra and ket vectors denote single configurations obtained by single excitations $p \rightarrow q$ and $r \rightarrow s$ from $\mathrm{M}_S = +1$ and -1 references, respectively. However, the nonorthogonality of alpha (or beta) MOs of bra and ket can arise some difficulties. Although one can compute the coupling terms by using a singular value decomposition of the overlap integral of the nonorthogonal molecular orbitals, we simply used the following spin-pairing coupling schemes in this work. We first define the two types of couplings can be defined by

$$H_{pq,rs}^{(k)\mathrm{intra}} \equiv \mathrm{sgn}(k)\,(ps\,|rq\,)\,, \tag{13a}$$

$$H_{pq,rs}^{(k)\mathrm{inter}} \equiv \mathrm{sgn}(k)\,\{(pq\,|rs\,) - (pr\,|sq\,)\}\,, \tag{13b}$$

with the sign function for the singlet and triplet states denoted as

$$\begin{aligned} \mathrm{sgn}(k) &= +1, \quad \text{if } k = S, \\ \mathrm{sgn}(k) &= -1, \quad \text{if } k = T. \end{aligned} \tag{14}$$

With these, the spin-pairing coupling are given by

$$\begin{aligned} A'^{(k)}_{pq,rs} = &(U^{(k)\mathrm{CO1}}_{pq} - U^{(k)\mathrm{CO2}}_{pq}) H^{(k)\mathrm{intra}}_{p\underline{\bar{q}},\bar{r}\underline{s}} (U^{(k)\mathrm{CO1}}_{rs} - U^{(k)\mathrm{CO2}}_{rs}) \\ &+ (U^{(k)\mathrm{O1V}}_{pq} - U^{(k)\mathrm{O2V}}_{pq}) H^{(k)\mathrm{intra}}_{\underline{p}\bar{q},\underline{\bar{r}}s} (U^{(k)\mathrm{O1V}}_{rs} - U^{(k)\mathrm{O2V}}_{rs}) \\ &+ U^{(k)\mathrm{CO1}}_{pq} H^{(k)\mathrm{inter}}_{\bar{p}\bar{q},\bar{r}\bar{s}} U^{(k)\mathrm{O2V}}_{rs} + U^{(k)\mathrm{CO2}}_{pq} H^{(k)\mathrm{inter}}_{\bar{p}\bar{q},\bar{r}\bar{s}} U^{(k)\mathrm{O1V}}_{rs} \\ &+ U^{(k)\mathrm{O1V}}_{pq} H^{(k)\mathrm{inter}}_{pq,rs} U^{(k)\mathrm{CO2}}_{rs} + U^{(k)\mathrm{O2V}}_{pq} H^{(k)\mathrm{inter}}_{pq,rs} U^{(k)\mathrm{CO1}}_{rs}, \end{aligned} \tag{15}$$

where $U^{(k)}_{pq}$ is the dimensional transformation matrix as described in Supporting Information. The bar notation used in the orbital indices is defined in Fig. 1(b), and the underline notation is defined as follows:

$$\begin{aligned} \underline{p} &\equiv O2, \quad \text{if } \; p = O1, \\ \underline{p} &\equiv O1, \quad \text{if } \; p = O2. \end{aligned} \tag{16}$$

Finally, the orbital Hessians for the singlet and triplet responses with the spin-pairing coupling is written by

$$A^{(k)}_{pq,rs} = A^{(k)(0)}_{pq,rs} + A'^{(k)}_{pq,rs}. \tag{17}$$

Orbital Reordering Scheme

Although the spatial parts of α and β UKS MOs tend to be similar to each other, they are not identical. To make matters worse, their relative orders are not guaranteed to be the same. If the MO shapes of χ_{O1} and χ_{O2} differ from those of $\bar{\chi}_{O1}$ and $\bar{\chi}_{O2}$, the dimensional transformation $U^{(k)}_{pq}$ and the spin pairing coupling in Eq. 12 become invalid. To address this challenge, MO reordering based on the maximum orbital overlap between α and β orbitals was implemented, ensuring that the α and β pair orbitals align accordingly.

However, MO reordering can potentially alter the corresponding response energies. This issue can be mitigated by preventing the exchange between occupied and virtual MOs. Specifically, for α MOs, the exchange between $O2$ and a is not allowed, and the exchange between $O1$ and i should be prohibited in the case of β MOs (Fig. 2). This restriction-based reordering only changes the phase of the reference state without affecting the energy of the reference state.

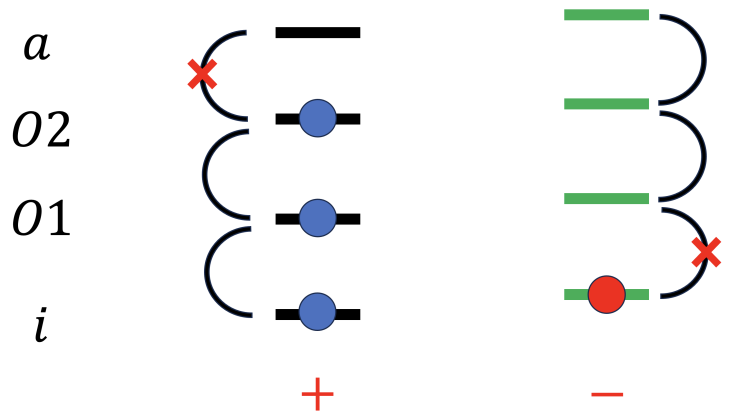

Figure 2: Schematic diagram of the orbital reordering scheme. Only rotations between α occupied orbitals and between β virtual orbitals are allowed, preserving the energy of both reference response states while possibly inducing phase changes.

Computation of $\langle \mathbf{S}^2 \rangle$

In wavefunction theory, the correct spin symmetry of the many-particle wavefunction can be enforced through proper construction.[62] For calculations performed using spin-unrestricted methods,[63] spin contamination of the wavefunction can be measured by identifying contributions with higher spin multiplicity. In the case of Density Functional Theory (DFT), only the Kohn-Sham (KS) reference wavefunction is available, which pertains to a fictitious reference system of non-interacting particles. Consequently, in principle, it is not possible to accurately calculate two-particle quantities such as $\langle \mathbf{S}^2 \rangle$, even if the exact KS reference wavefunction was known.

In spin-flip formalism, such as SF-TDDFT, spin contamination arises from the absence of specific configurations in the response space. Additionally, spin contamination from orbital asymmetries also occurs in unrestricted formulations. The MRSF formulation addresses this issue by including the missing configurations, thereby eliminating spin contamination from the response space. However, spin contamination due to orbital asymmetries can still persist. Unlike the Kohn-Sham (KS) molecular orbitals (MOs) in DFT, the wavefunction in response theories corresponds to an auxiliary wavefunction, which is the solution to the orbital Hessian matrix. As a result, the approximate expectation value of $\langle \mathbf{S}^2 \rangle$ can be obtained by applying the operator to the auxiliary wavefunction.

In the case of Restricted Open Kohn-Sham (ROKS), there is only one set of molecular orbitals (MOs). In contrast, for Unrestricted Kohn-Sham (UKS), the α and β MOs are different and not orthogonal, necessitating special attention. The detailed derivation of the approximate $\langle \mathbf{S}^2 \rangle$ formulation using the auxiliary wavefunction of Unrestricted Multi-Reference Spin-Flip (UMRSF) can be found in the Supporting Information. Here, we present the final equations.

With Casida's wavefunction ansatz,[64] the auxiliary wavefunction of MRSF-TDDFT is labeled as $\Psi_I^{(k)}$, where I denotes the I-th state in energy order within the manifold of the total spin quantum number ($k = S, T$). The $\Psi_I^{(k)}$ is expressed as a linear combination of configuration state functions (CSFs, $\Phi_{\text{Type}}^{(k)}$). There are four different types of CSFs originating from single spin-flip (de-)excitation in MRSF, abbreviated as OO, CO, OV, and a broken symmetry type CV. These types represent open-to-open, closed-to-open, open-to-virtual, and closed-to-virtual excitations, respectively. Depending on whether the state is a singlet or triplet, the OO type is represented as OS and OT, corresponding to combinations of open shell configurations for singlets and triplets, respectively.

With these notations, the singlet (S) and triplet (T) response states for $2N$-electron

systems can be represented as:

$$|\Psi_I^{(\mathrm{S})}\rangle = X_{\mathrm{G}}^{(\mathrm{S})}|\Phi_{\mathrm{G}}\rangle + X_{\mathrm{D}}^{(\mathrm{S})}|\Phi_{\mathrm{D}}\rangle + X_{\mathrm{OS}}^{(\mathrm{S})}|\Phi_{\mathrm{OS}}\rangle + \sum_{pq\in \mathrm{CO,OV,CV}} X_{pq}^{(\mathrm{S})}|\Phi_{pq}^{(S)}\rangle, \tag{18}$$

$$|\Psi_I^{(\mathrm{T})}\rangle = X_{\mathrm{OT}}^{(\mathrm{T})}|\Phi_{\mathrm{OT}}\rangle + \sum_{pq\in \mathrm{CO,OV,CV}} X_{pq}^{(\mathrm{T})}|\Phi_{pq}^{(T)}\rangle, \tag{19}$$

where the G and D configurations are the ground and doubly excited configurations of OO types, respectively. All the configuration functions (Φ) on the right-hand side of the equations are linear combinations of two Slater determinants derived from $M_S = \pm 1$ references ($|\psi^{\pm 1}\rangle$). For example, the configuration function of G is represented in a simple form as

$$|\Phi_{\mathrm{G}}\rangle = \frac{1}{2}(|\psi_{\mathrm{G}}^{+1}\rangle + |\psi_{\mathrm{G}}^{-1}\rangle) = \frac{1}{2}(||\phi_{\mathrm{C}}^{\alpha}\bar{\phi}_{\mathrm{C}}^{\beta}\phi_{\mathrm{O1}}^{\alpha}\bar{\phi}_{\mathrm{O1}}^{\beta}\rangle + ||\bar{\phi}_{\mathrm{C}}^{\alpha}\phi_{\mathrm{C}}^{\beta}\bar{\phi}_{\mathrm{O1}}^{\alpha}\phi_{\mathrm{O1}}^{\beta}\rangle), \tag{20}$$

where spin orbitals are defined by $\phi_p^{\sigma}(x) = \chi_p(\mathbf{r})\sigma(\theta)$ and $\bar{\phi}_p^{\sigma}(x) = \bar{\chi}_p(\mathbf{r})\sigma(\theta)$ with $\langle\chi_p|\chi_q\rangle = \langle\bar{\chi}_p|\bar{\chi}_q\rangle = \delta_{pq}$, $\langle\chi_p|\bar{\chi}_q\rangle = S_{pq}$, and $\sigma = \alpha, \beta$.

It should be emphasized that the spatial overlap $\langle\chi_p|\bar{\chi}_q\rangle$ between molecular orbitals from $M_S = \pm 1$ references is not zero, yielding S_{pq}. This is because they correspond to the overlaps between the spatial parts of α and β orbitals of UKS, respectively.

After rather involved derivations, the $\hat{S}^2$ expectation value for unnormalized singlet

and triplet states within the TLF0[65] approximation can be finally written as:

$$
\begin{aligned}
\langle \Psi_I^{(\mathrm{S})} | \hat{S}^2 | \Psi_I^{(\mathrm{S})} \rangle \simeq & \frac{1}{2} |X_{\mathrm{G}}^{(\mathrm{S})}|^2 [(n_\alpha - \sum_{p \in \mathrm{C,\,O1}} (S_{pp})^2) + (\prod_{p \in \mathrm{C,\,O1}} (S_{pp})^2)((n_\alpha - \sum_{p \in \mathrm{C,\,O1}} (S_{pp})^{-2}))] \\
& + \frac{1}{2} |X_{\mathrm{D}}^{(\mathrm{S})}|^2 [(n_\alpha - \sum_{p \in \mathrm{C,\,O2}} (S_{pp})^2) + (\prod_{p \in \mathrm{C,\,O2}} (S_{pp})^2)((n_\alpha - \sum_{p \in \mathrm{C,\,O2}} (S_{pp})^{-2}))] \\
& + |X_{\mathrm{OS}}^{(\mathrm{S})}|^2 [n_\alpha - \sum_{p \in \mathrm{C}} (S_{pp})^2 - \prod_{p \in \mathrm{C}} (S_{pp})^2] \\
& + \sum_{im \in \mathrm{CO}} |X_{im}^{(\mathrm{S})}|^2 [n_\alpha - \sum_{p \in \mathrm{C}} (S_{pp})^2 + (S_{ii})^2 - (S_{mm})^2 - \frac{(S_{mm})^2}{(S_{ii})^2} \prod_{p \in \mathrm{C}} (S_{pp})^2] \\
& + \sum_{ma \in \mathrm{OV}} |X_{ma}^{(\mathrm{S})}|^2 [n_\alpha - \sum_{p \in \mathrm{C}} (S_{pp})^2 - \prod_{p \in \mathrm{C}} (S_{pp})^2] \\
& + \sum_{ia \in \mathrm{CV}} |X_{ia}^{(\mathrm{S})}|^2 [n_\alpha - \sum_{p \in \mathrm{C}} (S_{pp})^2 + (S_{ii})^2 - \frac{1}{(S_{ii})^2} \prod_{p \in \mathrm{C}} (S_{pp})^2] \qquad (21)
\end{aligned}
$$

$$
\begin{aligned}
\langle \Psi_I^{(\mathrm{T})} | \hat{S}^2 | \Psi_I^{(\mathrm{T})} \rangle \simeq & |X_{\mathrm{OT}}^{(\mathrm{T})}|^2 [n_\alpha - \sum_{p \in \mathrm{C}} (S_{pp})^2 + \prod_{p \in \mathrm{C}} (S_{pp})^2] \\
& + \sum_{im \in \mathrm{CO}} |X_{im}^{(\mathrm{T})}|^2 [n_\alpha - \sum_{p \in \mathrm{C}} (S_{pp})^2 + (S_{ii})^2 - (S_{mm})^2 + \frac{(S_{mm})^2}{(S_{ii})^2} \prod_{p \in \mathrm{C}} (S_{pp})^2] \\
& + \sum_{ma \in \mathrm{OV}} |X_{ma}^{(\mathrm{S})}|^2 [n_\alpha - \sum_{p \in \mathrm{C}} (S_{pp})^2 + \prod_{p \in \mathrm{C}} (S_{pp})^2] \\
& + \sum_{ia \in \mathrm{CV}} |X_{ia}^{(\mathrm{S})}|^2 [n_\alpha - \sum_{p \in \mathrm{C}} (S_{pp})^2 + (S_{ii})^2 + \frac{1}{(S_{ii})^2} \prod_{p \in \mathrm{C}} (S_{pp})^2], \qquad (22)
\end{aligned}
$$

where n_α and n_β are number of α and β electrons. And S_{ij} is the overlap integral ($\langle \psi_{\mathrm{Type}}^{+1} | \psi_{\mathrm{Type}}^{-1} \rangle$) between molecular orbitals from $M_S = \pm 1$ references, which is not zero yielding S_{pq}.

Their normalization factors with TLF0[65] approximation are

$$\begin{aligned}\langle \Psi_I^{(\mathrm{S})} | \Psi_I^{(\mathrm{S})} \rangle &\simeq \frac{1}{2}|X_{\mathrm{G}}^{(\mathrm{S})}|^2(1+\prod_{p\in \mathrm{C,\,O1}}(S_{pp})^2)+\frac{1}{2}|X_{\mathrm{D}}^{(\mathrm{S})}|^2(1+\prod_{p\in \mathrm{C,\,O2}}(S_{pp})^2) \\ &\quad +|X_{\mathrm{OS}}^{(\mathrm{S})}|^2+\sum_{im\in \mathrm{CO}}|X_{im}^{(\mathrm{S})}|^2+\sum_{ma\in \mathrm{OV}}|X_{ma}^{(\mathrm{S})}|^2+\sum_{ia\in \mathrm{CV}}|X_{ia}^{(\mathrm{S})}|^2 \\ &= 1+\frac{1}{2}(\prod_{p\in \mathrm{C,\,O1}}(S_{pp})^2-1)+\frac{1}{2}(\prod_{p\in \mathrm{C,\,O2}}(S_{pp})^2-1) \qquad (23)\end{aligned}$$

$$\begin{aligned}\langle \Psi_I^{(\mathrm{T})} | \Psi_I^{(\mathrm{T})} \rangle &\simeq |X_{\mathrm{OT}}^{(\mathrm{T})}|^2+\sum_{im\in \mathrm{CO}}|X_{im}^{(\mathrm{T})}|^2+\sum_{ma\in \mathrm{OV}}|X_{ma}^{(\mathrm{T})}|^2+\sum_{ia\in \mathrm{CV}}|X_{ia}^{(\mathrm{T})}|^2 \\ &= 1 \qquad (24)\end{aligned}$$

Results and Discussions

The developed UMRSF method was benchmarked against three different systems, covering a wide range of problems including atomic multiplets, bond breaking, and Jahn-Teller distortion. The test calculations employed the BH&HLYP density functional[66–68] in conjunction with the 6-31G[69] or 6-31G(d) basis set, as noted below. The UMRSF-TDDFT and U-SF-TDDFT calculations with a collinear exchange-correlation (XC) kernel were performed using a local development version of the GAMESS-US program.

Recovering Degeneracy of Be Atom

Table 1: Ground state total energies (Hartree) and excitation energies (eV) for the Be atom using a 6-31G basis set. The values of $\langle \mathbf{S}^2 \rangle$ are given in parentheses in units of $\hbar^2$.

State	U-SF	UMRSF	RO-SF	RO-MRSF
^1S	-14.652321 (**0.0003**)	-14.652156 (**0.0000**)	-14.650997 (**0.0003**)	-14.650988 (**0.0000**)
^3P_z	2.874 (**1.9804**)	2.899 (**2.0000**)	2.877 (**1.9788**)	2.900 (**2.0000**)
$^3P_{x,y}$	3.676 (**1.0000**)	2.652 (**2.0000**)	3.688 (**1.0000**)	2.667 (**2.0000**)
^1P_z	4.924 (**0.0231**)	4.907 (**0.0000**)	4.935 (**0.0241**)	4.913 (**0.0000**)
$^1P_{x,y}$		4.668 (**0.0000**)		4.690 (**0.0000**)

It should be emphasized that both SF-TDDFT and MRSF-TDDFT can obtain the ground

singlet state as one of their response states, unlike TDDFT. This is because the ground singlet state can be obtained by a single excitation from their reference triplet state. The ground ^1S state of Be has the electron configuration of $1s^2 2s^2$. The low-lying excited states of Be include the triplet $^3P_{x,y,z}$ and singlet $^1P_{x,y,z}$, corresponding to the electron configuration of $1s^2 2s^2 p_k^1$, where $k = x, y, z$. As it is mostly described by a single closed-shell configuration, the energies obtained by the two theories are nearly identical to each other (-14.650997 vs. -14.650988 Hartree) with negligible spin-contamination in SF-TDDFT ($\langle \mathbf{S}^2 \rangle$ = 0.0003). U-SF-TDDFT and UMRSF yield nearly identical energy within $\sim$ 0.1 milli-Hartree for the ^1S ground electronic state. They are slightly reduced by $\sim$ milli-Hartree as compared to their RO counterparts, which can be attributed to the extra variational flexibility of UKS during the orbital optimization step.

The low-lying excited states of Be atom are described by the electron excitation from $2s \rightarrow 2p$. Within the context of MRSF theories, these particular excitations are combinations of $\alpha \rightarrow \beta$ spin-flip excitation of $2s\alpha$ and $\beta \rightarrow \alpha$ spin-flip excitation of $2s\beta$ as shown in

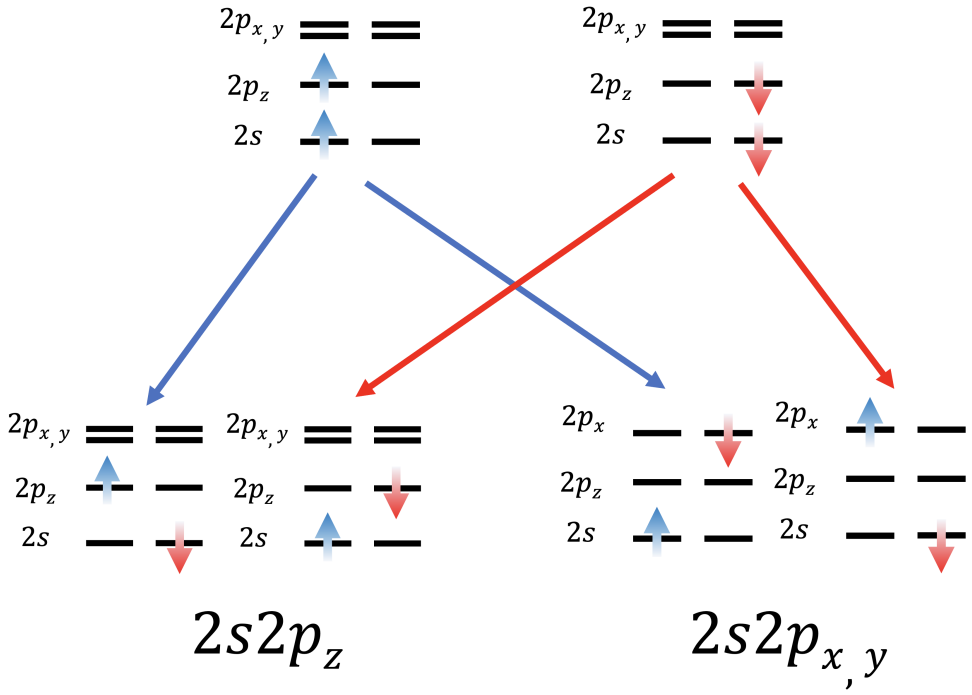

Figure 3: The $M_S = \pm 1$ reference triplet configurations (top) and the configurations that can be generated from them for the Be atom (bottom).

Fig. 3. The triplet reference utilizes $2p_z$ during orbital optimization, which breaks the orbital symmetries among the three $2p$ orbitals. The corresponding ^3P_z and ^1P_z state energies relative to the ground ^1S by UMRSF are 2.899 and 4.907 eV, respectively. On the other hand, MRSF produced corresponding values of 2.900 and 4.913 eV. Except for slight reductions in UMRSF, the two theories produced nearly identical values. The SF variants (U-SF and SF-TDDFT) exhibit relatively minor spin-contamination of the ^1Pz ($\langle \mathbf{S}^2 \rangle$ = 0.0231, 0.0241) and ^3Pz ($\langle \mathbf{S}^2 \rangle$ = 1.9804, 1.9788) components. As a result, their energies are in good agreement with those of MRSF variants within $\sim$ 0.02 eV.

However, the $^3Px,y$ and $^1Px,y$ components are completely mixed with each other in SF variants, resulting in a state energy of 3.676 and 3.688 eV with $\langle \mathbf{S}^2 \rangle$ = 1.0 (half-half mixture of singlet and triplet). As a result, it is not possible to assign their spin states. Normally, the $^3Px,y$ and ^3Pz states should be degenerate, as should the $^1Px,y$ and ^1Pz states. However, this exact spin-contamination has produced unphysical states. The same issue was observed in SF-TDDFT. In contrast, MRSF variants (UMRSF and MRSF) eliminated the spin contamination and produced state energies of 2.652 (2.667) eV and 4.668 (4.690) eV for $^3Px,y$ and $^1Px,y$, respectively. While these are not identical to the ^3Pz and ^1Pz energies, they are very close, within approximately 0.2 eV. Compared to the values from MRSF, all state energies in UMRSF are slightly reduced by about 0.01 eV, which is again attributed to the variational flexibility of UKS. It was discussed that the bulk of the slight splitting between the multiplet components is caused by the self-interaction error of the density functional.[28]

Bond-Breaking of HF molecule in Ground Electronic State

As mentioned earlier, the ability to generate the ground state as one of the response states allows for the study of bond-breaking reactions in the ground state, which has been one of the major limitations of DFT. As a simple test case, the bond breaking of hydrogen fluoride (HF) was investigated using UMRSF-TDDFT. The results, are presented in Fig. 4,

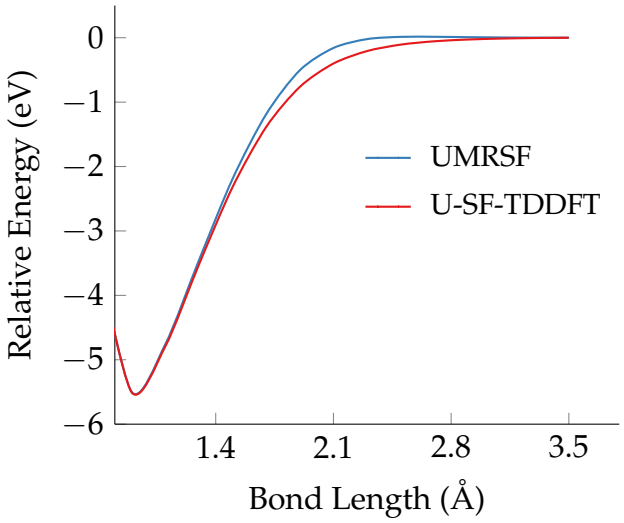

Figure 4: Potential energy curves (eV) of the $^1\Sigma^+$ singlet ground state of HF along the bond-stretching coordinate. The calculations employ the 6-31G basis set. The origin of the energy scale is chosen at the dissociation limit.

where the results of U-SF-TDDFT are also included for comparison.

The triplet $^3\Sigma^+$ state ($[\ldots \pi_x^2 \pi_y^2 \pi_z^1 \pi_z^{*1}]$) serves as the reference state from UKS. In the two limiting geometries of the bound singlet state at 0.9 Å and the dissociation limit, the two variants (SF and MRSF) exhibit nearly identical relative energies. This is because the bound state at 0.9 Å is essentially represented by a close-shell single configuration. At the dissociation limit, an exact singlet and triplet mixing ($\langle \mathbf{S}^2 \rangle = 1$) occurs in the U-SF-TDDFT. Since the interaction between the two separated electrons becomes nearly zero at this limit, the singlet and triplet states become energetically degenerate. Consequently, despite the exact singlet and triplet mixing, the final system energy of the U-SF-TDDFT is exactly identical to that of the UMRSF.

However, a clear difference appears near the bond length of 2.12 Å, where energy lowering of U-SF-TDDFT by 0.23 eV is seen. (see also Table 2) Relevant orbitals of HF dissociations are the three p of Fluorine and s of hydrogen orbitals as shown in Fig. 5(a). The φ_3 and φ_6 correspond to the bonding and antibonding combinations of HF molecule, while φ_4 and φ_5 are entirely p orbitals of Fluorine. At the bound state with bond length of 0.9 Å, the three orbitals of φ_3, φ_4 and φ_5 are all doubly occupied, which is described

the **D** configuration of Fig. 5(b). In the dissociation limit, the two singly occupied φ_4 and φ_6 as represented by the configurations of **L** and **R** dominate with some other minor contributions. In the middle of the breaking with bond length of 2.12 Å, these two sets

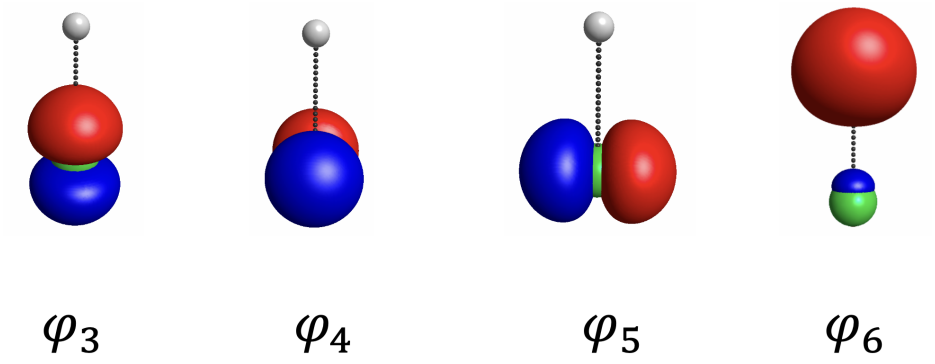

(a)

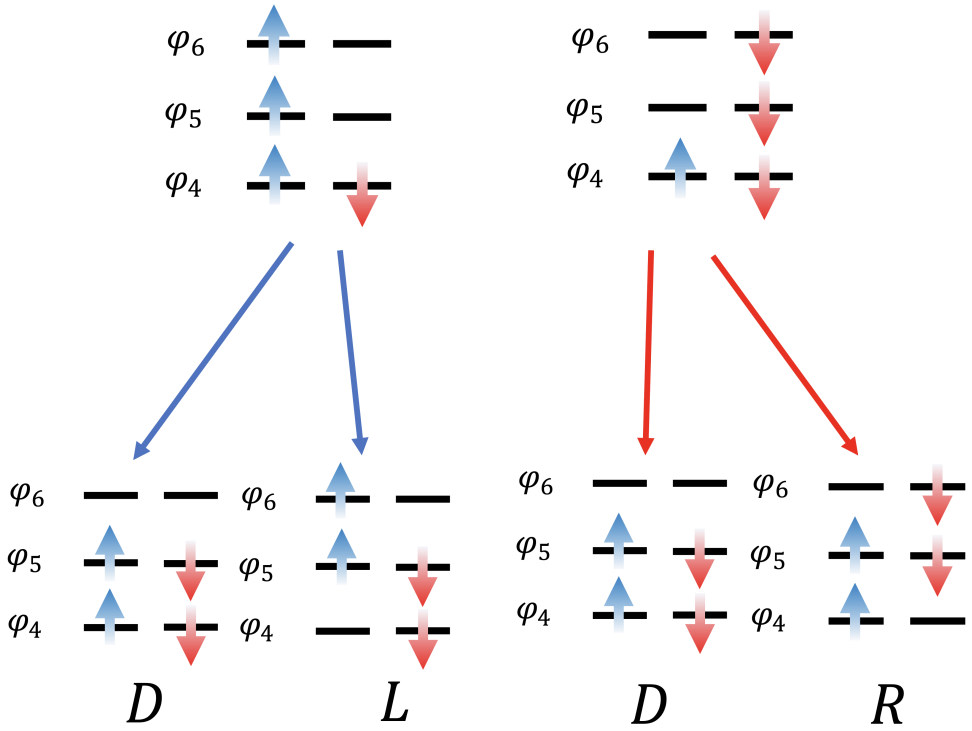

(b)

Figure 5: (a) Relevant molecular orbitals and (b) electronic configurations of references and responses of hydrogen fluoride.

of configurations contribute together as summarized in Table 2. As the configurations of **L** and **R** dominate, the missing **R** in the case of U-SF-TDDFT inevitably introduces the significant spin-contamination yielding lower state energy. It appears U-SF-TDDFT relies more on **L** than **D** configurations as compared to UMRSF counterpart, which introduces the mixing with triplet state. On the other hand, the $\langle \mathbf{S}^2 \rangle$ of UMRSF is 0.02, nearly eliminates the spin-contamination.

Table 2: Relative energies at the bond length of 2.12 Å with respect to the most stable structures of Hydrogen Fluoride, calculated using BHHLYP with a 6-31G basis set. The D and L/R represent the coefficients of the configurations shown in Fig. 5. The values of $\langle \mathbf{S}^2 \rangle$ are given in parentheses in units of $\hbar^2$.

Method	Rel. E (eV)	**D**	**L/R**	$\langle \mathbf{S}^2 \rangle$
UMRSF	0.31	0.60	-0.80	0.02
U-SF-TDDFT	0.08	0.56	-0.83 (Missing **R**)	0.76

Jahn-Teller Distortions in *tri*-Methylene Methane (TMM) Diradical

Single-reference methods of such as conventional Kohn-Sham (KS) DFT methods,[1] fail to accurately describe the singlet-triplet (ST) gaps because they cannot properly account for diradicals. Diradicals are molecules with two unpaired electrons occupying two (nearly) degenerate molecular orbitals (open-shells).[70–76] When the two unpaired electrons in a diradical[77] are (nearly) independent of each other, the triplet ${}^3A_2^{'}$ becomes the ground state, as seen in the trimethylenemethane diradical (TMM) in Fig. 6b (following Hund's rules).[78]

The high spin components ($M_S = \pm 1$) of the triplet state are well approximated by a single electronic configuration. However, the theoretical description of the $M_S = 0$ component of the triplet and the open-shell singlet (OSS) state, essential ingredients for diradicals, requires at least two electronic configurations with two singly occupied orbitals (the $1a_2$ and $2b_1$ in Fig. 6b, respectively). Again, the ability to generate the ground state as one of the response states by SF and MRSF variants plays a big role in producing

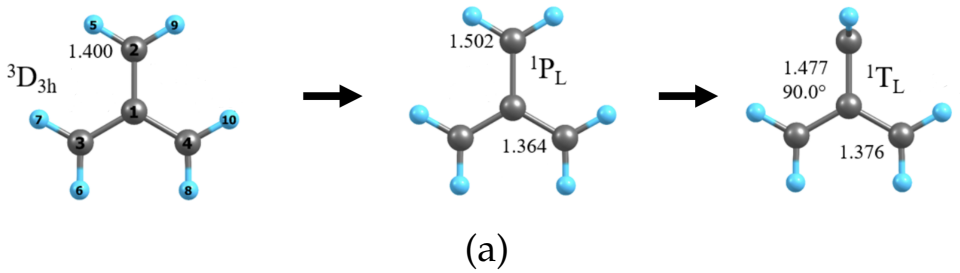

(a)

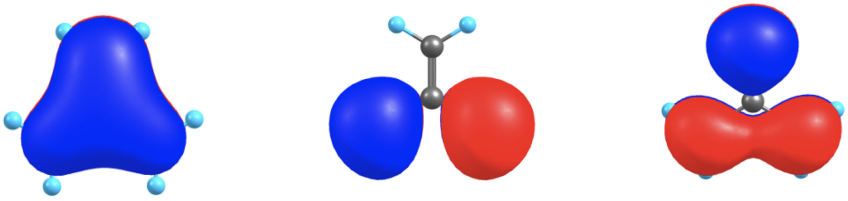

(b)

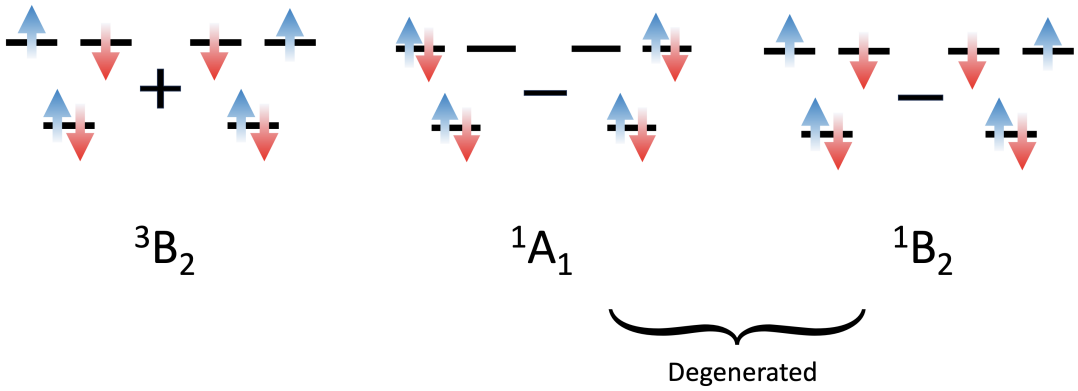

(c)

Figure 6: (a) The D_{3h}, ^1P_L, and ^1T_L structures of trimethylenemethane (TMM). (b) Two SOMOs ($1a_2$, $2b_1$) and HOMO-1 ($1b_1$) molecular orbitals. Orbitals are labeled with C2v labels. (c) Major configurations that contribute to $M_S = 0$ of triplet and singlet states of TMM as generated by MRSF.

the necessary configurations for the proper description of diradicals. In the case of TMM, the negative combination of doubly occupied ground and doubly excited configurations, $^1A_1$, becomes degenerate with $^1B_2$ at its highest symmetry of D_{3h}, providing the main driving force of the Jahn-Teller distortions.

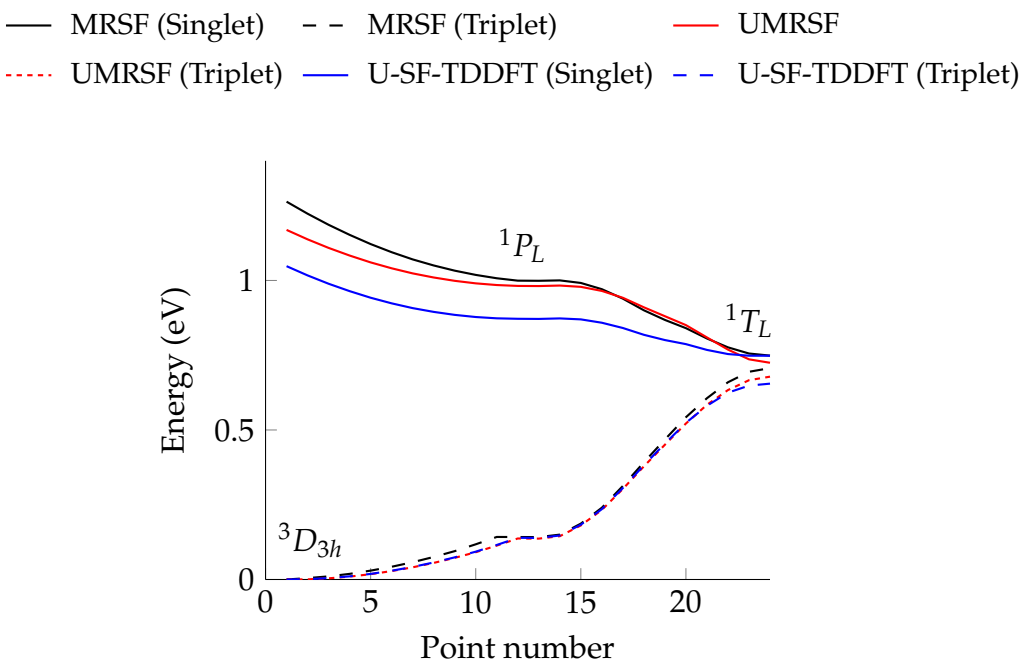

Figure 7: Potential energy surfaces along $D_{3h} \rightarrow {}^1P_L \rightarrow {}^1T_L$ by MRSF, UMRSF, and U-SF-TDDFT for TMM. The geometries were optimized by MRSF/BH&HLYP/6-31G(d).

In the singlet state, the degeneracy of the $^1B_2$ and $^1A_1$ states at the D_{3h} geometry is lifted by the lengthening of one or two C–C bonds (δ) and the torsion (φ) of one of the carbene groups along the respective C–C bond. By lengthening the two bottom C–C bonds occupied by the anti-bonding molecular orbital (MO) ($1a_2$), the $^1A_1$ state is stabilized compared to $^1B_2$. On the other hand, lengthening the top single C–C bond stabilizes $1b_1$, and so does $^1B_2$, leading to the ^1P_L geometry. Finally, torsion (φ) produces ^1T_L, as shown in Fig. 6a. Accordingly, the potential energy surfaces (PESs) of $D_{3h} \rightarrow {}^1P_L \rightarrow {}^1T_L$ by MRSF, UMRSF, and U-SF-TDDFT are generated by geodesic interpolations along the three points based on optimized geometries by MRSF (Fig. 7).

The degenerate $^1B_2$ and $^1A_1$ states with a triplet ground state occur from all calculations

by MRSF, UMRSF, and U-SF-TDDFT at D_{3h} geometry. The relative singlet energy compared to the triplet by UMRSF and U-SF-TDDFT is lower by 0.1 and 0.2 eV than that of MRSF-TDDFT, respectively. The reduction in UMRSF energy is due to spatial orbital relaxations, while that of U-SF-TDDFT additionally comes from spin-contamination. These state energy lowerings appear across the entire surfaces. The singlet $^1B_2$ state becomes degenerate with the ground triplet state at the ^1T_L geometry, as the mixing of triplet contamination does not change its state energy.

Conclusions

An unrestricted version of Mixed-Reference Spin-Flip Time-Dependent Density Functional Theory (UMRSF-TDDFT) was developed based on unrestricted Kohn-Sham orbitals (UKS), providing extra orbital flexibility to the existing MRSF-TDDFT.

The spatial asymmetries in the α and β Kohn-Sham MOs require special attention as they are not identical to each other. Furthermore, their relative orders are also not guaranteed to be the same. To address this challenge, an MO reordering scheme based on the maximum orbital overlap between α and β orbitals was implemented, ensuring that the α and β pair orbitals align accordingly.

After obtaining fully relaxed UKS MOs from variational SCF, the MO reordering scheme is applied before the response part of the computation. Since MO reordering can potentially alter the corresponding response energies, our scheme prevents the MO exchange between occupied and virtual spaces, which changes the phase of the reference state without affecting the reference energy of UKS. Furthermore, we obtained the approximate $\langle \mathbf{S}^2 \rangle$ values of UMRSF using the auxiliary wave function and measured the degree of spin contamination in UMRSF.

In an application to the ground and excited states of a Be atom, the ground ^1S energy calculated by UMRSF is slightly reduced by approximately a milli-Hartree compared to

its RO counterpart, which can be attributed to the extra variational flexibility of UKS during the orbital optimization step. UMRSF produced state energies of 2.652 eV and 4.668 eV for ${}^3P_{x,y}$ and ${}^1P_{x,y}$, respectively. While these are not identical to the ${}^3P_z$ and ${}^1P_z$ energies, they are very close, within approximately 0.2 eV, effectively recovering the state degeneracy.

A clear difference between UMRSF and U-SF-TDDFT in the bond breaking of the hydrogen fluoride system appears near a bond length of 2.12 Å, where the energy of U-SF-TDDFT is reduced by 0.23 eV due to spin contamination.

In the case of trimethylenemethane (TMM), the negative combination of doubly occupied ground and doubly excited configurations, ${}^1A_1$, becomes degenerate with ${}^1B_2$ at its highest symmetry of D_{3h}, which is the main driving force behind the Jahn-Teller distortions. Along the distortion potential energy surfaces (PESs) from D_{3h} to ${}^1P_L$ to ${}^1T_L$ as calculated by MRSF, UMRSF, and U-SF-TDDFT, the relative singlet energy compared to the triplet is lower by 0.1 and 0.2 eV for UMRSF and U-SF-TDDFT, respectively, than that of MRSF-TDDFT. The reduction in UMRSF energy is attributed to spatial orbital relaxations, whereas the reduction in U-SF-TDDFT energy results from spin contamination.

In summary, the additional orbital relaxations afforded by unrestricted Kohn-Sham (UKS) orbitals in UMRSF result in lower total system energies compared to their restricted open-shell counterparts. This provides extra electron correlation to the MRSF theories, thereby expanding the applicability of MRSF theory to more challenging multi-configurational systems. This improvement enhances the robustness and accuracy of MRSF, making it a versatile tool for studying a wide range of complex electronic structures.

Acknowledgements

This work was supported by the NRF funded by the Ministry of Science and ICT (2020R1A2C2008246 and 2020R1A5A1019141 to C.H.C.) for the applications of developed theories. Work

by M.O. and S.L. was funded by the New Faculty Startup Fund from Seoul National University.

Supporting Information Available

A detailed derivation of dimensional transformation and $\langle \mathbf{S}^2 \rangle$ for UMRSF-TDDFT are given in a separate Supporting Information file.

References

(1) Squires, R. R.; Cramer, C. J. Electronic interactions in aryne biradicals. Ab initio calculations of the structures, thermochemical properties, and singlet- triplet splittings of the didehydronaphthalenes. *J. Phys. Chem. A* **1998**, *102*, 9072–9081.

(2) Lee, S.; Horbatenko, Y.; Filatov, M.; Choi, C. H. Fast and Accurate Computation of Nonadiabatic Coupling Matrix Elements Using the Truncated Leibniz Formula and Mixed-Reference Spin-Flip Time-Dependent Density Functional Theory. *J. Phys. Chem. Lett.* **2021**, *12*, 4722–4728.

(3) Dreuw, A.; Weisman, J. L.; Head-Gordon, M. Long-range charge-transfer excited states in time-dependent density functional theory require non-local exchange. *The Journal of chemical physics* **2003**, *119*, 2943–2946.

(4) Dreuw, A.; Head-Gordon, M. Single-reference ab initio methods for the calculation of excited states of large molecules. *Chemical reviews* **2005**, *105*, 4009–4037.

(5) Dev, P.; Agrawal, S.; English, N. J. Determining the appropriate exchange-correlation functional for time-dependent density functional theory studies of charge-transfer excitations in organic dyes. *The Journal of Chemical Physics* **2012**, *136*, 224301.

(6) Maitra, N. T. Undoing static correlation: Long-range charge transfer in time-dependent density-functional theory. *The Journal of chemical physics* **2005**, *122*, 234104.

(7) Baerends, E.; Gritsenko, O.; Van Meer, R. The Kohn–Sham gap, the fundamental gap and the optical gap: the physical meaning of occupied and virtual Kohn–Sham orbital energies. *Physical Chemistry Chemical Physics* **2013**, *15*, 16408–16425.

(8) Cave, R. J.; Zhang, F.; Maitra, N. T.; Burke, K. A dressed TDDFT treatment of the 2^1A_g states of butadiene and hexatriene. *Chemical Physics Letters* **2004**, *389*, 39–42.

(9) Neugebauer, J.; Baerends, E. J.; Nooijen, M. Vibronic coupling and double excitations in linear response time-dependent density functional calculations: Dipole-allowed states of N_2. *The Journal of chemical physics* **2004**, *121*, 6155–6166.

(10) Maitra, N. T.; Zhang, F.; Cave, R. J.; Burke, K. Double excitations within time-dependent density functional theory linear response. *The Journal of Chemical Physics* **2004**, *120*, 5932–5937.

(11) Park, W.; Shen, J.; Lee, S.; Piecuch, P.; Filatov, M.; Choi, C. H. Internal Conversion between Bright ($1^1B_u^+$) and Dark ($2^1A_g^-$) States in s-trans-Butadiene and s-trans-Hexatriene. *J. Phys. Chem. Lett.* **2021**, *12*, 9720–9729.

(12) Aryasetiawan, F.; Gunnarsson, O.; Rubio, A. Excitation energies from time-dependent density-functional formalism for small systems. *EPL (Europhysics Letters)* **2002**, *57*, 683.

(13) Filatov, M. Ensemble DFT approach to excited states of strongly correlated molecular systems. *Density-functional methods for excited states* **2015**, 97–124.

(14) Levine, B. G.; Ko, C.; Quenneville, J.; Martínez, T. J. Conical intersections and double excitations in time-dependent density functional theory. *Molecular Physics* **2006**, *104*, 1039–1051.

(15) Huix-Rotllant, M.; Filatov, M.; Gozem, S.; Schapiro, I.; Olivucci, M.; Ferré, N. Assessment of density functional theory for describing the correlation effects on the ground and excited state potential energy surfaces of a retinal chromophore model. *Journal of chemical theory and computation* **2013**, *9*, 3917–3932.

(16) Gozem, S.; Melaccio, F.; Valentini, A.; Filatov, M.; Huix-Rotllant, M.; Ferré, N.; Frutos, L. M.; Angeli, C.; Krylov, A. I.; Granovsky, A. A. et al. Shape of multireference, equation-of-motion coupled-cluster, and density functional theory

potential energy surfaces at a conical intersection. *Journal of chemical theory and computation* **2014**, *10*, 3074–3084.

(17) Ferré, N.; Filatov, M.; Huix-Rotllant, M.; Adamo, C. *Density-functional methods for excited states*; Springer, 2016; Vol. 368.

(18) Nikiforov, A.; Gamez, J. A.; Thiel, W.; Huix-Rotllant, M.; Filatov, M. Assessment of approximate computational methods for conical intersections and branching plane vectors in organic molecules. *J. Chem. Phys.* **2014**, *141*, 124122.

(19) Tuna, D.; Lefrancois, D.; Wolański, Ł.; Gozem, S.; Schapiro, I.; Andruniów, T.; Dreuw, A.; Olivucci, M. Assessment of Approximate Coupled-Cluster and Algebraic-Diagrammatic-Construction Methods for Ground- and Excited-State Reaction Paths and the Conical-Intersection Seam of a Retinal-Chromophore Model. *J. Chem. Theory Comput.* **2015**, *11*, 5758–5781.

(20) Shavitt, I. In *Modern Theoretical Chemistry Vol. 3: Methods of Electronic Structure Theory*; Schaefer III, H. F., Ed.; Plenum: New York, 1977; pp 189–275.

(21) Karwowski, J. A.; Shavitt, I. In *Handbook of Molecular Physics and Quantum Chemistry*; Wilson, S., Ed.; Wiley: Chichester, U.K., 2003; Vol. 2; pp 227–271.

(22) Szalay, P. G.; Müller, T.; Gidofalvi, G.; Lischka, H.; Shepard, R. Multiconfiguration Self-Consistent Field and Multireference Configuration Interaction Methods and Applications. *Chem. Rev.* **2012**, *112*, 108–181.

(23) Roos, B. O. In *Ab Initio Methods in Quantum Chemistry II*; Lawley, K. P., Ed.; John Wiley and Sons: New York, 1987; pp 399–446.

(24) Andersson, K.; Malmqvist, P.; Roos, B. O. Second order perturbation theory with a complete active space self consistent field reference function. *J. Chem. Phys.* **1992**, *96*, 1218–1226.

(25) Yarkony, D. R. In *Conical Intersections. Electronic Structure, Dynamics and Spectroscopy*; Domcke, W., Yarkony, D. R., Köppel, H., Eds.; Advanced series in physical chemistry; World Scientific: Singapore, 2004; Vol. 15; pp 41–127.

(26) Lischka, H.; Dallos, M.; Szalay, P. G.; Yarkony, D. R.; Shepard, R. Analytic evaluation of nonadiabatic coupling terms at the MR-CI level. I. Formalism. *J. Chem. Phys.* **2004**, *120*, 7322–7329.

(27) Dallos, M.; Lischka, H.; Shepard, R.; Yarkony, D. R.; Szalay, P. G. Analytic evaluation of nonadiabatic coupling terms at the MR-CI level. II. Minima on the crossing seam: Formaldehyde and the photodimerization of ethylene. *J. Chem. Phys.* **2004**, *120*, 7330–7339.

(28) Lee, S.; Filatov, M.; Lee, S.; Choi, C. H. Eliminating spin-contamination of spin-flip time dependent density functional theory within linear response formalism by the use of zeroth-order mixed-reference (MR) reduced density matrix. *J. Chem. Phys.* **2018**, *149*, 104101.

(29) Lee, S.; Kim, E. E.; Nakata, H.; Lee, S.; Choi, C. H. Efficient implementations of analytic energy gradient for mixed-reference spin-flip time-dependent density functional theory (MRSF-TDDFT). *J. Chem. Phys.* **2019**, *150*, 184111.

(30) Horbatenko, Y.; Lee, S.; Filatov, M.; Choi, C. H. Performance Analysis and Optimization of Mixed-Reference Spin-Flip Time-Dependent Density Functional Theory (MRSF-TDDFT) for Vertical Excitation Energies and Singlet–Triplet Energy Gaps. *J. Phys. Chem. A* **2019**, *123*, 7991–8000.

(31) Horbatenko, Y.; Lee, S.; Filatov, M.; Choi, C. H. How Beneficial Is the Explicit Account of Doubly-Excited Configurations in Linear Response Theory? *J. Chem. Theory Comput.* **2021**, *17*, 975–984.

(32) Horbatenko, Y.; Sadiq, S.; Lee, S.; Filatov, M.; Choi, C. H. Mixed-Reference Spin-Flip Time-Dependent Density Functional Theory (MRSF-TDDFT) as a Simple yet Accurate Method for Diradicals and Diradicaloids. *J. Chem. Theory Comput.* **2021**, *17*, 848–859.

(33) Baek, Y. S.; Lee, S.; Filatov, M.; Choi, C. H. Optimization of Three State Conical Intersections by Adaptive Penalty Function Algorithm in Connection with the Mixed-Reference Spin-Flip Time-Dependent Density Functional Theory Method (MRSF-TDDFT). *J. Phys. Chem. A* **2021**, *125*, 1994–2006.

(34) Park, W.; Lee, S.; Huix-Rotllant, M.; Filatov, M.; Choi, C. H. Impact of the Dynamic Electron Correlation on the Unusually Long Excited-State Lifetime of Thymine. *J. Phys. Chem. Lett.* **2021**, *12*, 4339–4346.

(35) Lee, S.; Shostak, S.; Filatov, M.; Choi, C. H. Conical Intersections in Organic Molecules: Benchmarking Mixed-Reference Spin–Flip Time-Dependent DFT (MRSF-TD-DFT) vs Spin–Flip TD-DFT. *J. Phys. Chem. A* **2019**, *123*, 6455.

(36) Lee, S.; Kim, E.; Lee, S.; Choi, C. H. Fast Overlap Evaluations for Nonadiabatic Molecular Dynamics Simulations: Applications to SF-TDDFT and TDDFT. *J. Chem. Theory Comput.* **2019**, *15*, 882.

(37) Horbatenko, Y.; Lee, S.; Filatov, M.; Choi, C. H. Performance Analysis and Optimization of Mixed-Reference Spin-Flip Time-Dependent Density Functional Theory (MRSF-TDDFT) for Vertical Excitation Energies and Singlet–Triplet Energy Gaps. *J. Phys. Chem. A* **2019**, *123*, 7991.

(38) Pomogaev, V.; Lee, S.; Shaik, S.; Filatov, M.; Choi, C. H. Exploring Dyson's Orbitals and Their Electron Binding Energies for Conceptualizing Excited States from Response Methodology. *J. Phys. Chem. Lett.* **2021**, *12*, 9963–9972.

(39) Kim, H.; Park, W.; Kim, Y.; Filatov, M.; Choi, C. H.; Lee, D. Relief of excited-state antiaromaticity enables the smallest red emitter. *Nat. Commun.* **2021**, *12*, 1–9.

(40) Lee, S.; Park, W.; Nakata, H.; Filatov, M.; Choi, C. H. Recent advances in ensemble density functional theory and linear response theory for strong correlation. *Bull. Korean Chem. Soc.* **2022**, *43*, 17–34.

(41) Park, W.; Shen, J.; Lee, S.; Piecuch, P.; Joo, T.; Filatov, M.; Choi, C. H. Dual Fluorescence of Octatetraene Hints at a Novel Type of Singlet-to-Singlet Thermally Activated Delayed Fluorescence Process. *J. Phys. Chem. C* **2022**,

(42) Park, W.; Filatov, M.; Sadiq, S.; Gerasimov, I.; Lee, S.; Joo, T.; Choi, C. H. A Plausible Mechanism of Uracil Photohydration Involves an Unusual Intermediate. *J. Phys. Chem. Lett.* **2022**, *13*, 7072–7080.

(43) Huix-Rotllant, M.; Schwinn, K.; Pomogaev, V.; Farmani, M.; Ferré, N.; Lee, S.; Choi, C. H. Photochemistry of thymine in solution and DNA revealed by an electrostatic embedding QM/MM combined with mixed-reference spin-flip TDDFT. *Journal of Chemical Theory and Computation* **2022**,

(44) Lee, S.; Park, W.; Nakata, H.; Filatov, M.; Choi, C. H. *Time-Dependent Density Functional Theory*; Jenny Stanford Publishing, 2023; pp 101–139.

(45) Shostak, S.; Park, W.; Oh, J.; Kim, J.; Lee, S.; Nam, H.; Filatov, M.; Kim, D.; Choi, C. H. Ultrafast Excited State Aromatization in Dihydroazulene. *Journal of the American Chemical Society* **2023**,

(46) Sadiq, S.; Park, W.; Mironov, V.; Lee, S.; Filatov, M.; Choi, C. H. Prototropically Controlled Dynamics of Cytosine Photodecay. *The Journal of Physical Chemistry Letters* **2023**, *14*, 791–797.

(47) Komarov, K.; Park, W.; Lee, S.; Zeng, T.; Choi, C. H. Accurate Spin–Orbit Coupling by Relativistic Mixed-Reference Spin-Flip-TDDFT. *Journal of Chemical Theory and Computation* **2023**, *19*, 953–964.

(48) Park, W.; Alías-Rodríguez, M.; Cho, D.; Lee, S.; Huix-Rotllant, M.; Choi, C. H. Mixed-reference spin-flip time-dependent density functional theory for accurate x-ray absorption spectroscopy. *Journal of Chemical Theory and Computation* **2022**, *18*, 6240–6250.

(49) Japahuge, A.; Lee, S.; Choi, C. H.; Zeng, T. Design of singlet fission chromophores with cyclic (alkyl)(amino) carbene building blocks. *J. Chem. Phys.* **2019**, *150*, 234306.

(50) Pradhan, E.; Lee, S.; Choi, C. H.; Zeng, T. Diboron-and diaza-doped anthracenes and phenanthrenes: their electronic structures for being singlet fission chromophores. *J. Phys. Chem. A* **2020**, *124*, 8159–8172.

(51) James, D.; Pradhan, E.; Lee, S.; Choi, C. H.; Zeng, T. Dicarbonyl anthracenes and phenanthrenes as singlet fission chromophores. *Can. J. Chem.* **2022**, *99*, 1–10.

(52) Park, W.; Komarov, K.; Lee, S.; Choi, C. H. Mixed-Reference Spin-Flip Time-Dependent Density Functional Theory: Multireference Advantages with the Practicality of Linear Response Theory. *J. Phys. Chem. Lett.* **2023**, *14*, 8896–8908.

(53) Park, W.; Lashkaripour, A.; Komarov, K.; Lee, S.; Huix-Rotllant, M.; Choi, C. H. Toward Consistent Predictions of Core/Valence Ionization Potentials and Valence Excitation Energies by MRSF-TDDFT. *Journal of Chemical Theory and Computation* **2024**,

(54) Li, Z.; Liu, W. Theoretical and numerical assessments of spin-flip time-dependent density functional theory. *The Journal of chemical physics* **2012**, *136*, 024107.

(55) Wang, F.; Ziegler, T. Time-dependent density functional theory based on a noncollinear formulation of the exchange-correlation potential. *The Journal of chemical physics* **2004**, *121*, 12191–12196.

(56) Shao, Y.; Head-Gordon, M.; Krylov, A. I. The spin–flip approach within time-dependent density functional theory: Theory and applications to diradicals. *The Journal of chemical physics* **2003**, *118*, 4807–4818.

(57) Hennefarth, M. R.; Hermes, M. R.; Truhlar, D. G.; Gagliardi, L. Linearized Pair-Density Functional Theory. *Journal of Chemical Theory and Computation* **2023**, *19*, 3172–3183.

(58) Zhang, X.; Herbert, J. M. Spin-flip, tensor equation-of-motion configuration interaction with a density-functional correction: A spin-complete method for exploring excited-state potential energy surfaces. *The Journal of Chemical Physics* **2015**, *143*, 234107.

(59) Runge, E.; Gross, E. K. Density-functional theory for time-dependent systems. *Physical review letters* **1984**, *52*, 997.

(60) Casida, M. E.; Chong, D. Recent advances in density functional methods. *Computational Chemistry: Reviews of Current Trends* **1995**,

(61) Casida, M. E.; Huix-Rotllant, M. Progress in time-dependent density-functional theory. *Annual review of physical chemistry* **2012**, *63*, 287–323.

(62) Roothaan, C. C. J. New Developments in Molecular Orbital Theory. *Reviews of Modern Physics* **1960**, *32*, 179.

(63) Pople, J. A.; Nesbet, R. K. Self-Consistent Orbitals for Radicals. *Journal of Chemical Physics* **1954**, *22*, 571.

(64) Casida, M. E. *Recent Advances In Density Functional Methods: (Part I)*; World Sci., 1995; pp 155–192.

(65) Lee, S.; Horbatenko, Y.; Filatov, M.; Choi, C. H. Fast and Accurate Computation of Nonadiabatic Coupling Matrix Elements Using the Truncated Leibniz Formula and Mixed-Reference Spin-Flip Time-Dependent Density Functional Theory. *The Journal of Physical Chemistry Letters* **2021**, *12*, 4722–4728.

(66) Becke, A. D. Density-functional exchange-energy approximation with correct asymptotic behavior. *Physical review A* **1988**, *38*, 3098.

(67) Lee, C.; Yang, W.; Parr, R. G. Development of the Colle-Salvetti correlation-energy formula into a functional of the electron density. *Physical Review B* **1988**, *37*, 785.

(68) Becke, A. D. A new mixing of Hartree–Fock and local density–functional theories. *The Journal of Chemical Physics* **1993**, *98*, 1372–1377.

(69) Pople, J. A.; Krishnan, R. G. High-level ab initio calculations of the valence electronic structure of molecules. 1. Computational procedures. *International Journal of Quantum Chemistry* **1980**, *S14*, 545–560.

(70) Borden, W. T. Reevaluating the Concept of Diradicals. *Accounts of Chemical Research* **2015**, *48*, 2741–2748.

(71) Abe, M. Diradicals. *Chemical Reviews* **2013**, *113*, 7011–7088.

(72) Peng, C.; Mazziotti, D. A. Variational Two-Electron Reduced-Density-Matrix-Driven Approaches for Strongly Correlated Systems. *The Journal of Chemical Physics* **2012**, *137*, 134112.

(73) Y. Yang, S. M.; Chan, G. K.-L. Singlet and Triplet Energy Gaps of Diradicals from Spin-Flip Density Functional Theory. *Journal of Chemical Theory and Computation* **2015**, *11*, 4606–4616.

(74) Rajca, A. Organic Diradicals and Polyradicals: From Spin Coupling to Magnetism? *Chemical Reviews* **1994**, *94*, 871–893.

(75) Gryn'ova, L. A.; Coote, M. L. The Theory and Application of Electron Paramagnetic Resonance to Diradicals. *Chemical Society Reviews* **2015**, *44*, 1522–1546.

(76) Abe, M. Chemistry of Stable Singlet Diradicals. *Journal of Synthetic Organic Chemistry, Japan* **2012**, *70*, 1050–1061.

(77) Karplus, M.; Fraenkel, G. K. Diradicals. *Annual Review of Physical Chemistry* **1972**, *23*, 397–430.

(78) Hund, F. Zur Deutung der Molekelspektren. I. *Zeitschrift für Physik* **1925**, *33*, 345–371.